Materials Characterization 136 (2018) 111–121

Contents lists available at ScienceDirect

Materials Characterization

journal homepage: www.elsevier.com/locate/matchar

Micro- and macro-scale characterization of nano-SiO_2 reinforced alkali activated slag composites

Wu-Jian Long*, Bing-Xu Xiao, Yu-Cun Gu, Feng Xing

Guangdong Provincial Key Laboratory of Durability for Marine Civil Engineering, Shenzhen Durability Center for Civil Engineering, College of Civil Engineering, Shenzhen University, Shenzhen 518060, Guangdong, PR China

ARTICLE INFO

Keywords:
Alkali activated slag cement composites
X-ray computed tomography
Nanoindentation
SEM-EDS
Microstructure

ABSTRACT

The effect of nano-SiO_2 on the micromechanical properties and microstructure of alkali-activated slag cement (AASC) composites was investigated. The investigation involved the use of: (i) nanoindentation to determine the elastic properties of the constituent phases using statistical deconvolution; (ii) scanning electron microscopy equipped with energy-dispersive X-ray spectroscopy and backscattered electrons to identify and characterize the solid phases in the microstructure; and (iii) X-ray computed tomography microscopy to determine the morphology of microscale pores and mercury intrusion porosimetry to measure the volume fraction of the nanoscale pores. The combined use of micro- and macro-scale characterization tools can establish a logical link between the macro-mechanics, microstructure, and micromechanical properties, which provides valuable information aiding the material design of AASC with nanoparticles.

1. Introduction

Approximately 3.6 billion tons of CO_2 is produced worldwide each year, where 10% of all emissions is the result of the production of ordinary Portland cement (OPC). Meanwhile, the proportion of CO_2 in the greenhouse gases is up to 65% [1]. The development and utilization of low-carbon and environment-friendly cementitious materials are the inevitable choice for the sustainable development of green building materials. Alkali-activated cement (AAC) is a new type of green cement-based material, produced by the reaction between the potential water-hardened materials (e.g., slag, fly ash, and metakaolin) with pozzolanic activity and alkaline activators (e.g., NaOH and Na_2SiO_3) [2,3]. Compared to OPC, AAC uses volcanic cementitious material to replace cement, thus reducing CO_2 emissions from the overall process [4]. Moreover, several studies have reported better mechanical properties and durability of AAC compared to OPC [5,6].

Applications of nanotechnology in modern concrete technology have been widely considered as the main research direction for developing ultrahigh-performance concrete [7]. Several studies conducted on the effects of nanoparticles on concrete properties have shown that the introduction of nanoparticles can improve the mechanical properties of cement-based materials [8–11]. Several groups have performed systematic studies on the mechanical properties and micro-performance of cement-based materials doped with nanoparticles. Behfarnia and Rostami [12], Senff et al., [13] and Riahi and Nazari [14] confirmed that nano-SiO_2 (NS) can easily combine with and fill the pores between the hydration products in the alkali-activated slag cement (AASC) matrix. The compressive strength values were shown to increase with increasing nano-SiO_2 (NS) content in the range of 0–3% (of the mass of binder) [12]. However, the compressive strength decreased as the NS content reached 5% [12,14].

The effect of NS on the microscale performance of AASC can be quantitatively characterized by nanoindentation techniques. In addition, the micromechanical properties of the various internal phases can be obtained by nanoindentation technology [15], and cement-based and alkali-activated materials have been extensively studied using this technique [16–21]. Nemecek et al. [22] applied the statistical nanoindentation technique (SNT) to the polymerization products of alkali-activated fly ash using different curing methods. The results indicated that four phases with different elastic modulus values existed in the matrix. Das et al. [20] carried out a nanoindentation study on alkali-activated slag material and concluded that the homogenized Young's modulus originating from SNT was in good agreement with the experimental macro-scale Young's modulus.

Both AAC and OPC are inherently porous and heterogeneous structures; therefore, the mechanical and sustainable properties of material are closely related to the microstructure and pore structure [23]. Thus, characterization of these properties is a critical step in understanding the material properties. Mercury intrusion porosimetry (MIP) is a common technique for observing the internal porous

* Corresponding author at: College of Civil Engineering, Shenzhen University, Shenzhen 518060, PR China.
E-mail address: longwj@szu.edu.cn (W.-J. Long).

https://doi.org/10.1016/j.matchar.2017.12.013
Received 25 September 2017; Received in revised form 23 November 2017; Accepted 11 December 2017
Available online 12 December 2017
1044-5803/

Table 1
Chemical composition of slag (%).

Component	CaO	SiO_2	Al_2O_3	MgO	TiO_2	Fe_2O_3	MnO	Na_2O	LOI
Content	39.08	35.12	14.20	8.47	0.71	0.62	0.69	0.98	0.13

structure of cement-based materials, and is widely used in the statistical analysis of internal pores of alkali-activated materials [24–26]. MIP has some drawbacks, such as assumption of pore shapes, inconsistencies in pressurized mercury intrusion, and poor description of the phase connectivity. These limitations can be overcome to a large extent through the use of X-ray computed tomography microscopy (XCT) techniques [20]. XCT can provide valuable information in the analysis of pore networks in OPC and AAC [27], and has been employed in the analysis of the pore structure of cementitious materials. Synchrotron microtomography is considered highly suitable for the evaluation of the pore structure that influences the transport properties and material durability [28–31].

Recently, studies regarding AAC mainly focused on the alkali-activated slag (AASC), alkali-activated fly ash (AAFA), and alkali-activated metakaolin cementitious (AAMC) materials. In general, alkali activation agents are favorable for enhancing the early-age mechanical properties since the activity of the slag is higher than that of the fly ash. In addition, unlike AAFA, AASC does not require high temperatures during early-age curing; therefore, in this study, AASC was selected as the research material. It has been found that doping of NS in the AASC matrix promotes the formation of polymerization products; thus, the micromorphology and micromechanical properties were improved [12]. In this study, the microstructure and micromechanical properties of NS-AASC were systematically investigated using a combination of advanced microscale measurements, establishing a logical relationship between the macromechanical and micromechanical properties. The effects of NS on the micromechanical properties of the various phases of AASC (calcium silicate hydrate and sodium aluminosilicate hydrate (C(N−A)−S−H), and partly activated and non-activated particles) were investigated using nanoindentation. Both MIP and XCT were used to investigate the effect of NS on the pore structures at the microscale and nanoscale. The effect of NS on the mechanical properties of AASC was studied by scanning electron microscopy (SEM), back-scattered electron (BSE) microscopy, and energy dispersive X-ray spectroscopy (EDS) micro-measurement techniques. The combination of the microstructure and micromechanical properties of heterogeneous materials can be used to predict the macromechanical properties and provides an efficient approach for optimizing the material design and mechanical properties of AASC. Moreover, these advanced techniques can also open up avenues for performance prediction of similar materials.

Table 2
Mix proportions of AASC (kg/m^3).

Mix no.	Slag	Sodium silicate	NaOH	Water	NS
0NS	1320.65	172.42	28.17	428.76	0
2NS	1154.88	150.78	24.63	321.20	76.80

Note: 0NS = 0% of NS in cement (by mass); 2NS = 2% of NS replacement in cement (by mass).

2. Experimental Programs

2.1. Materials and Procedure

2.1.1. Raw Materials

A S95 ground granulated blast-furnace slag was used which conformed to Chinese Standard GB/T18046 [32] with a specific surface area of 430 m^2/kg and density of 2.90 g/cm^3. The chemical composition of this slag is shown in Table 1. A mixture of solid NaOH and sodium silicate (Na_2SiO_3 with 14.30 wt% Na_2O, 28.00 wt% SiO_2, and 57.70 wt% H_2O) was used as the alkali activator. The NaOH was an analytically pure reagent. The modulus Ms (molar ratio of Na_2O to SiO_2) of liquid sodium was 2.0.

The colloidal NS was a uniform silica dispersion with a solid particle content of 30 wt% and a size range of 8–24 nm. To avoid re-agglomeration of the nanoparticles, the colloidal NS was ultrasonically dispersed at 400 W and 28 KHz in water for 10 min. Atomic force microscopy (AFM) indicated that after dispersion, the NS particles were not agglomerated, as shown in Fig. 1(a)–(b). The maximum height of the particles in Fig. 1 is 21.4 nm, with a range of 8–24 nm, indicating that the nanoparticles were well dispersed.

2.1.2. Mix Proportions

The water/binder (W/B) ratio of the AASC in this investigation was 0.4, which was determined after comprehensively considering the workability (230 mm, conforming to the Chinese standard of GB/T2419 [33]) and strength (60 MPa at 28 days) of AASC according to previous investigations. An alkali activator with a Na_2O concentration of 4.0% (by mass of slag) and Ms of 1.2 was used. The water in the activator and the NS solution was deducted from the total amount of water. Previous findings [12,14] indicated that approximately 2 wt% NS doping can contribute to better mechanical properties of AASC; therefore, this doping content was selected for the subsequent experiments. Details of the mixtures are listed in Table 2. Note that the focus of this investigation was not the development of the AASC mixtures, but the use of combined characterization techniques for property prediction.

The well-dispersed NS solution and water were added to the alkaline solution, and mixed for 2 min with a glass stirring rod. Then, the

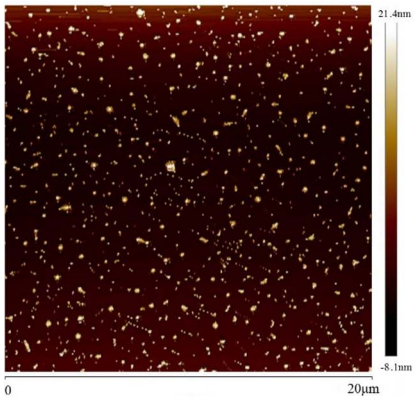

(a) The characteristics by AFM

(b) The well dispersed NS solution

Fig. 1. The NS characteristics. (a) The characteristics by AFM; (b) the well dispersed NS solution.